

## ORIGINAL ARTICLE

NCOA3 coactivator is a transcriptional target of XBP1 and regulates PERK–eIF2 $\alpha$ –ATF4 signalling in breast cancerA Gupta<sup>1</sup>, MM Hossain<sup>1</sup>, N Miller<sup>2</sup>, M Kerin<sup>2</sup>, G Callagy<sup>1</sup> and S Gupta<sup>1</sup>

XBP1 is a multitasking transcription factor and a key component of the unfolded protein response (UPR). Despite the wealth of knowledge about the role of XBP1 in luminal/ER-positive breast cancer, not much is known about the effectors of XBP1 in this context. Here we show that NCOA3 is a transcriptional target of XBP1. We observed increased expression of NCOA3 during conditions of UPR and oestrogen (E2) stimulation. Further investigations revealed a role for the IRE1–XBP1 axis in the induction of NCOA3 during UPR and oestrogen signalling. We identify a novel role for NCOA3 in activation of PERK–ATF4 axis during UPR where knockdown of NCOA3 compromised the optimal activation of the PERK–ATF4 pathway. We found that NCOA3 is required for induction of XBP1 during E2 stimulation and uncover a positive feedback regulatory loop that maintains high levels of NCOA3 and XBP1 in breast cancer. Furthermore, upregulated NCOA3 was required for XBP1-mediated resistance to antihormonal agents. Increased expression of NCOA3 was associated with poor prognosis and higher levels of XBP1-S in breast cancer tissues. Our results uncover a novel steroid hormone-independent role for NCOA3 in UPR signalling. Further we identify a positive feedback regulatory loop consisting of XBP1 and NCOA3 that maintains high levels of NCOA3 and XBP1 expression in breast cancer tissues. Taken together our data identify XBP1–NCOA3 axis that regulates cell fate decisions in ER-positive breast cancer cells.

*Oncogene* (2016) 35, 5860–5871; doi:10.1038/onc.2016.121; published online 25 April 2016

## INTRODUCTION

Physiological or pathological processes that disturb protein folding in the endoplasmic reticulum activate a set of signalling pathways termed as the unfolded protein response (UPR). This concerted and complex cellular response is mediated by three molecular sensors, PKR-like ER kinase (PERK), activated transcription factor 6 (ATF6) and inositol-requiring enzyme 1 (IRE1) present in the membrane of endoplasmic reticulum.<sup>1</sup> The luminal domain of PERK, IRE1 and ATF6 interacts with the endoplasmic reticulum chaperone glucose-regulated protein 78 (GRP78). However, upon accumulation of unfolded proteins, GRP78 dissociates from these molecules, leading to their activation. The most salient feature of UPR is to increase the functional activity of a variety of transcription factors (ATF6, ATF4, XBP1 and CHOP). Once activated, these transcription factors coordinate transcriptional induction of genes encoding for endoplasmic reticulum-resident chaperones, endoplasmic reticulum-associated degradation machinery, amino acid transport and metabolism proteins, phospholipid biosynthesis enzymes and several others, including many that have no obvious direct relationship to secretory pathway function.<sup>1,2</sup>

Invasive breast cancer is a heterogeneous disease with varied molecular features, behaviour and response to therapy. Oestrogen receptor  $\alpha$  (ER) is the primary therapeutic target in breast cancer and is expressed in 70% of cases. Endocrine therapy is the mainstay of treatment for patients with advanced ER-positive breast cancer. One-third of women treated with hormonal therapy for 5 years will have recurrent disease within 15 years, and therefore endocrine-resistant disease may constitute up to one-quarter of all breast cancers.<sup>3</sup> The Cancer Genome Atlas (TCGA) consortium reported that most dominant feature of Luminal/ER-

positive breast cancers is increased mRNA and protein levels of ESR1, GATA3, FOXA1, XBP1 and MYB. Most notably ESR1 and XBP1 were highly expressed and infrequently mutated.<sup>4</sup> The expression of XBP1-S mRNA and protein can be upregulated following 17 $\beta$ -estradiol (E2) treatment of ER-positive human breast cancer cell lines.<sup>5,6</sup> XBP1 physically interacts with ER and potentiates ER-dependent transcriptional activity in a ligand-independent manner.<sup>7</sup> Ectopic expression of XBP1-S in ER-positive breast cancer cells can lead to oestrogen-independent growth and reduced sensitivity to antioestrogens.<sup>8</sup> Downregulation of XBP1 reduces the survival of transformed human cells under hypoxic conditions and impairs their ability to grow as tumour xenografts in SCID mice.<sup>9</sup> Thus accumulating evidence suggests an active role of the IRE1–XBP1 pathway in oestrogen signalling.<sup>10</sup> Despite the wealth of knowledge about the role of XBP1-S in luminal/ER-positive breast cancer not much is known about the molecular effectors (transcriptional targets) of XBP1-S in context of oestrogen signalling.

Nuclear receptor coactivator 3 (NCOA3/SRC-3/AIB1/ACTR/pCIP/RAC3) is a member of p160 family of coactivators.<sup>11</sup> It is an oncogenic coactivator and interacts with nuclear receptors (NRs) to enhance the expression of cognate target genes.<sup>12</sup> By modulating gene expression, NCOA3 regulates diverse physiological functions and has been implicated in the development of breast cancer.<sup>13</sup> Transgenic mice-overexpressing NCOA3 shows increased mammary epithelial cell proliferation, development of mammary hyperplasia and tumorigenesis.<sup>11</sup> The ablation of NCOA3 in mouse mammary tumour virus (MMTV)/v-Ha-ras mice suppresses mammary gland ductal hyperplasia and mammary gland tumorigenesis.<sup>14</sup> NCOA3 not only functions to promote

<sup>1</sup>Discipline of Pathology, School of Medicine, Lambe Institute for Translational Research, National University of Ireland, Galway, Ireland and <sup>2</sup>Discipline of Surgery, School of Medicine, Clinical Science Institute, National University of Ireland, Galway, Ireland. Correspondence: Professor S Gupta, Discipline of Pathology, School of Medicine, Clinical Science Institute, National University of Ireland, H91 REW4, Galway, Ireland.

E-mail: sanjeev.gupta@nuigalway.ie

Received 24 October 2015; revised 25 January 2016; accepted 29 February 2016; published online 25 April 2016

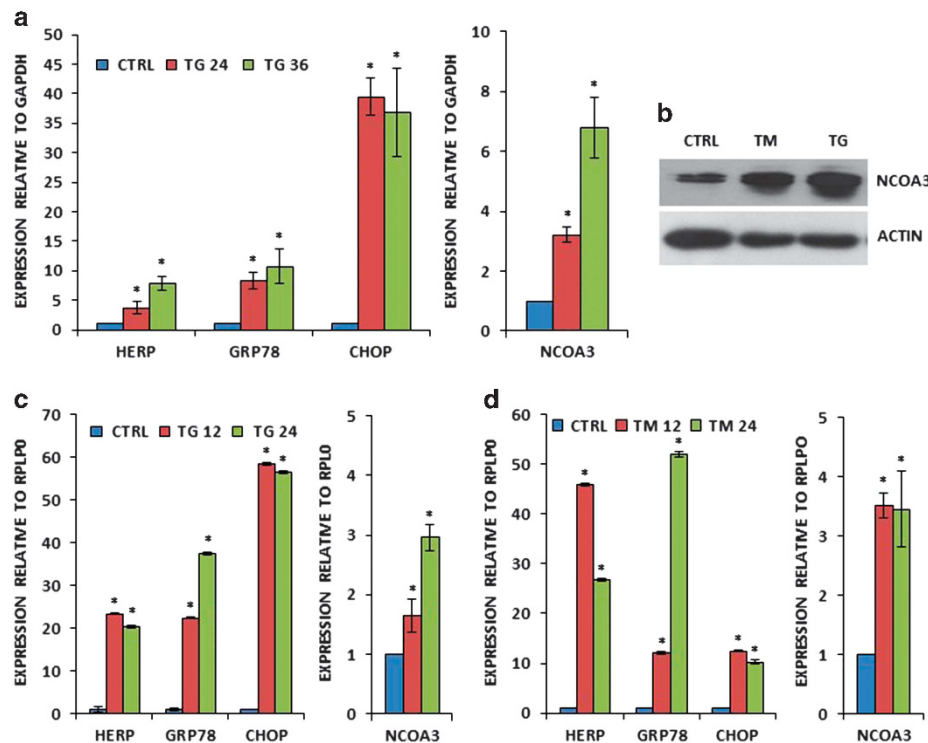


**Figure 1.** Increased expression of NCOA3 by UPR in human breast cancer cells. **(a)** MCF7 cells were either untreated (CTRL) or treated with (1.0  $\mu$ M) TG for indicated time points. The expression level of UPR-responsive genes (GRP78, HERP and CHOP) and NCOA3 was quantified by real-time RT-PCR, normalizing against GAPDH. Error bars represent mean  $\pm$  s.d. from three independent experiments performed in triplicate. **(b)** MCF7 cells were either untreated (CTRL) or treated with (1.0  $\mu$ M) TG and (1.0  $\mu$ g/ml) TM for 24 h. Western blotting of total protein was performed using antibodies against NCOA3 and  $\beta$ -actin. **(c, d)** T47D cells were either untreated (CTRL) or treated with (1.0  $\mu$ M) TG **(c)** and (1.0  $\mu$ g/ml) TM **(d)** for indicated time points. The expression level of UPR-responsive genes (GRP78, HERP and CHOP) and NCOA3 was quantified by real-time RT-PCR, normalizing against RPLP0. Error bars represent mean  $\pm$  s.d. from three independent experiments performed in triplicate. \* $P$  < 0.05, two-tailed unpaired *t*-test compared with untreated cells.

breast cancer development, it also participates in resistance to antihormonal therapy.<sup>15</sup> Increased expression of NCOA3 is strongly correlated with shorter disease-free and overall survival.<sup>16</sup> NCOA3 was found to be overexpressed in >60% of primary breast tumours; however its gene is amplified in only 5–10% of breast cancers.<sup>17,18</sup> Nonetheless, how NCOA3 becomes overexpressed in breast cancers is not well understood.

In this study we demonstrate that expression of NCOA3 is regulated by XBP1-S during the conditions of UPR, as well as oestrogen stimulation in human breast cancer cells. We show that inhibition of IRE1 activity and knockdown of XBP1 expression both compromised the induction of NCOA3 during UPR and oestrogen signalling. Our results describe an important non-NR function of NCOA3 where IRE1-XBP1-dependent upregulation of NCOA3 regulates optimal activation of the PERK-ATF4 axis during UPR. We also show that NCOA3 is required for induction of XBP1 and cellular proliferation upon oestrogen stimulation. Higher expression of NCOA3 was associated with poor prognosis and mRNA levels of NCOA3 correlated with spliced XBP1 transcript levels in breast cancer tissues. These findings provide novel insights into the biological function of XBP1 in ER-positive breast cancer.

## RESULTS

Upregulation of NCOA3 expression during conditions of UPR

During the analysis of the microarray gene expression data set (GSE63252) we found that expression of NCOA3 was robustly induced (logFC >2) upon treatment with two different pharmacological inducers of endoplasmic reticulum (EnR) stress. To

experimentally assess if UPR upregulates NCOA3 gene expression in breast cancer cells, MCF7 and T47D cells were exposed to different EnR stressors: N-linked glycosylation inhibitor tunicamycin (TM) and ER Ca-ATPase family (SERCA) inhibitor thapsigargin (TG).<sup>19</sup> TG increased the expression of HERP, GRP78, CHOP (bonafide UPR-responsive genes) and NCOA3 mRNA levels in a time-dependent manner (Figure 1a). We observed an increase in NCOA3 protein upon treatment with TG and TM of MCF7 cells (Figure 1b). Next we treated T47D cells with TG and TM. We observed a significant increase in the expression of HERP, GRP78, CHOP (bonafide UPR-responsive genes) and NCOA3 mRNA levels in TG and TM-treated T47D cells (Figures 1c and d). In order to confirm that regulation of NCOA3 during EnR stress was not restricted to ER-positive breast cancer cells, we examined levels of NCOA3 during conditions of EnR stress in MDA-MB231 cells. We observed a significant increase in the expression of HERP, GRP78, CHOP (bonafide UPR-responsive genes) and NCOA3 mRNA levels in bortezomib-treated MDA-MB231 cells (Supplementary Figure S1).

Induction of NCOA3 during EnR stress is dependent on the IRE1-XBP1 axis

Next we investigated the role of PERK and IRE1 arms of the UPR in the regulation of the NCOA3 expression. MCF7 cells were treated with TG alone or in combination with the GSK-PERK inhibitor<sup>20</sup> and (4 $\mu$ 8C and STF083010) IRE1 inhibitors.<sup>21,22</sup> As shown in Figure 2a, 4 $\mu$ 8C and STF083010 efficiently attenuated the TG-induced production of spliced XBP1. Further we observed that GSK-PERK inhibitor (PI) abrogated the TG-induced

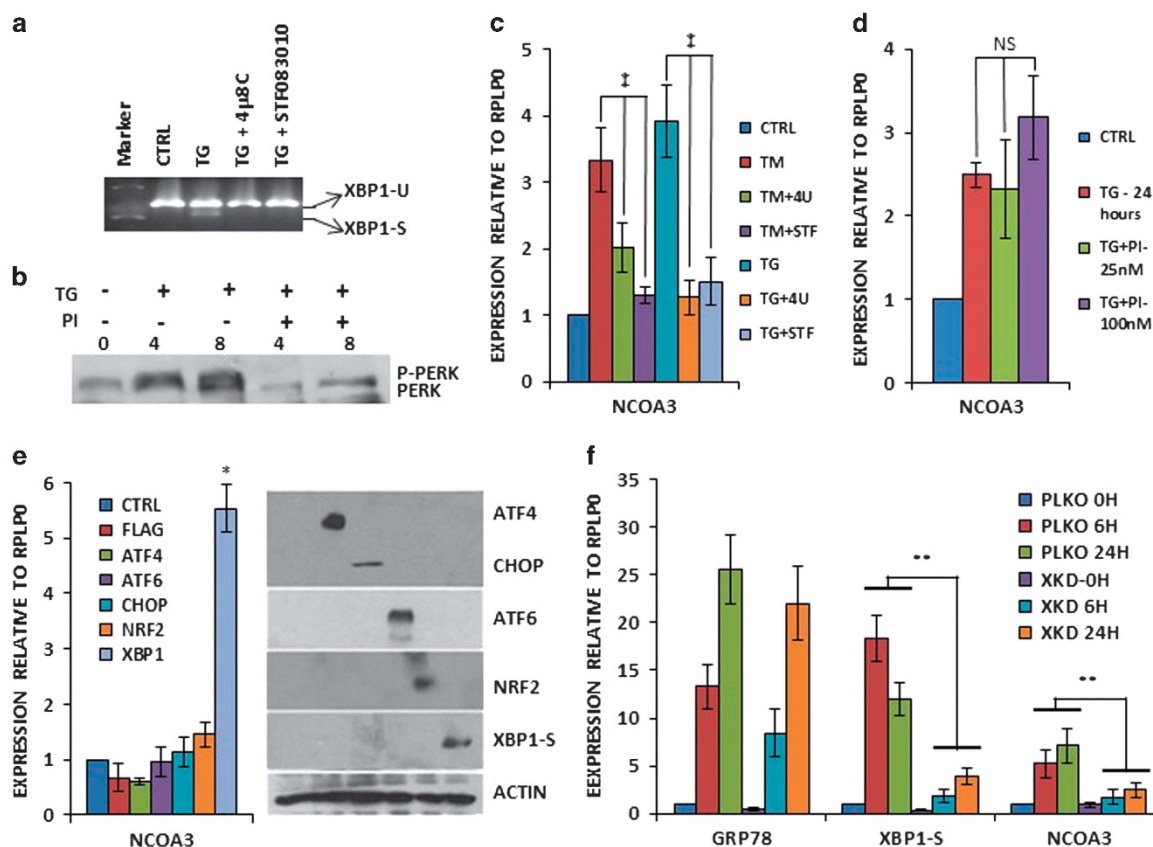


**Figure 2.** Upregulation of NCOA3 during UPR is mediated by the IRE1–XBP1 pathway. **(a)** MCF7 cells were either untreated (CTRL) or treated with (1.0  $\mu$ M) TG in the absence and presence of IRE1 inhibitors, (10  $\mu$ M) 4 $\mu$ 8C (4 U) and (100  $\mu$ M) STF083010 (STF) for 24 h. Cells were harvested and expression of XBP1 (unspliced and spliced) was analysed by RT–PCR followed by gel electrophoresis. **(b)** MCF7 cells were treated with TG (1.0  $\mu$ M) in the absence and presence of (25 nM) GSK-PERK inhibitor (PI) for indicated time points. Whole-cell lysates were subjected to sodium dodecyl sulphate–polyacrylamide gel electrophoresis (SDS–PAGE) followed by immunoblotting using PERK antibody. **(c)** MCF7 cells were either untreated (CTRL) or treated with TG (1.0  $\mu$ M) and (1.0  $\mu$ g/ml) TM in the absence and presence of IRE1 inhibitors as in **(a)**, and the expression level of NCOA3 was quantified by real-time RT–PCR, normalizing against RPLP0. Error bars represent mean  $\pm$  s.d. from three independent experiments performed in triplicate. **(d)** MCF7 cells were either untreated (CTRL) or treated with (1.0  $\mu$ M) TG in the absence and presence of (25 nM) GSK-PERK inhibitor (PI) for 24 h. The expression level of NCOA3 was quantified by real-time RT–PCR, normalizing against RPLP0. Error bars represent mean  $\pm$  s.d. from three independent experiments performed in triplicate. **(e)** MCF7 cells were transfected with (CTRL) pcDNA3-FLAG or plasmids expressing indicated UPR transcription factors (ATF4, ATF6, CHOP, NRF2 and XBP1-S). Cells were harvested 24 h post transfection normalizing against RPLP0. Error bars represent mean  $\pm$  s.d. from three independent experiments performed in triplicate. Equivalent amounts of cell lysates were resolved by SDS–PAGE and immunoblotting was performed using antibodies against FLAG, ATF4, spliced XBP1 and  $\beta$ -actin. ATF4, CHOP and NRF2 are FLAG-tagged.  $\beta$ -Actin served as a loading control. **(f)** MCF7-control (PLKO) and MCF7-XBP1 knockdown (XKD) cells were treated with (1.0  $\mu$ M) TG for indicated time points. The expression levels of GRP78, XBP1-S and NCOA3 was quantified by real-time RT–PCR, normalizing against RPLP0. Error bars represent mean  $\pm$  s.d. from three independent experiments performed in triplicate. \* $P$  < 0.05, two-tailed unpaired  $t$ -test compared with untreated cells;  $\ddagger P$  < 0.05 for one-way ANOVA; \*\* $P$  < 0.05, two-tailed unpaired  $t$ -test comparing respective time points; NS, not significant at  $P$  < 0.05.

auto-phosphorylation of PERK (Figure 2b). These results confirmed that both PERK and IRE1 inhibitors were blocking their respective targets. We observed that both 4 $\mu$ 8C and STF083010 compromised the TG and TM-mediated increase in the expression of NCOA3 (Figure 2c), whereas GSK-PERK inhibitor (PI) had no effect on TG-mediated increase in the expression of NCOA3 (Figure 2d). To determine which mammalian UPR transcriptional activators regulate NCOA3 expression, we transfected MCF7 cells with plasmids encoding indicated gene products (Figure 2e). These ectopic transcription factors were functional and regulated the expression of their cognate target genes (Supplementary SF2). We observed that ectopic expression of spliced XBP1 resulted in a significant increase in the NCOA3 transcripts level (Figure 2e). To further confirm the role of XBP1 in the induction of NCOA3, we generated the control (MCF7-PLKO) and XBP1 knockdown subclones (MCF7-XKD) of MCF7 cells. For this purpose we tested a panel of XBP1-targeting shRNAs for their knockdown

efficiency (Supplementary SF3). MCF7 cells were transduced with pLKO.1-Puro or XBP1-targeting shRNAs (TRCN0000019805) lentiviruses followed by puromycin selection to obtain control (MCF7-PLKO) and XBP1 knockdown subclones (MCF7-XKD) of MCF7 cells. We found that XBP1 knockdown clones were compromised in the induction of spliced XBP1 and NCOA3 upon TG treatment (Figure 2f). The knockdown of XBP1 did not alter the induction of GRP78 upon TG treatment (Figure 2f). Collectively, these results suggest that induction of NCOA3 during UPR is dependent on the IRE1–XBP1 axis.

NCOA3 is a transcriptional target of XBP1

Examination of the nucleotide sequence of human NCOA3 promoter showed a sequence homologous to the consensus XBP1-binding site at nucleotide position –119 to –98 relative to the transcriptional start site (Figure 3a). A NCOA3 promoter

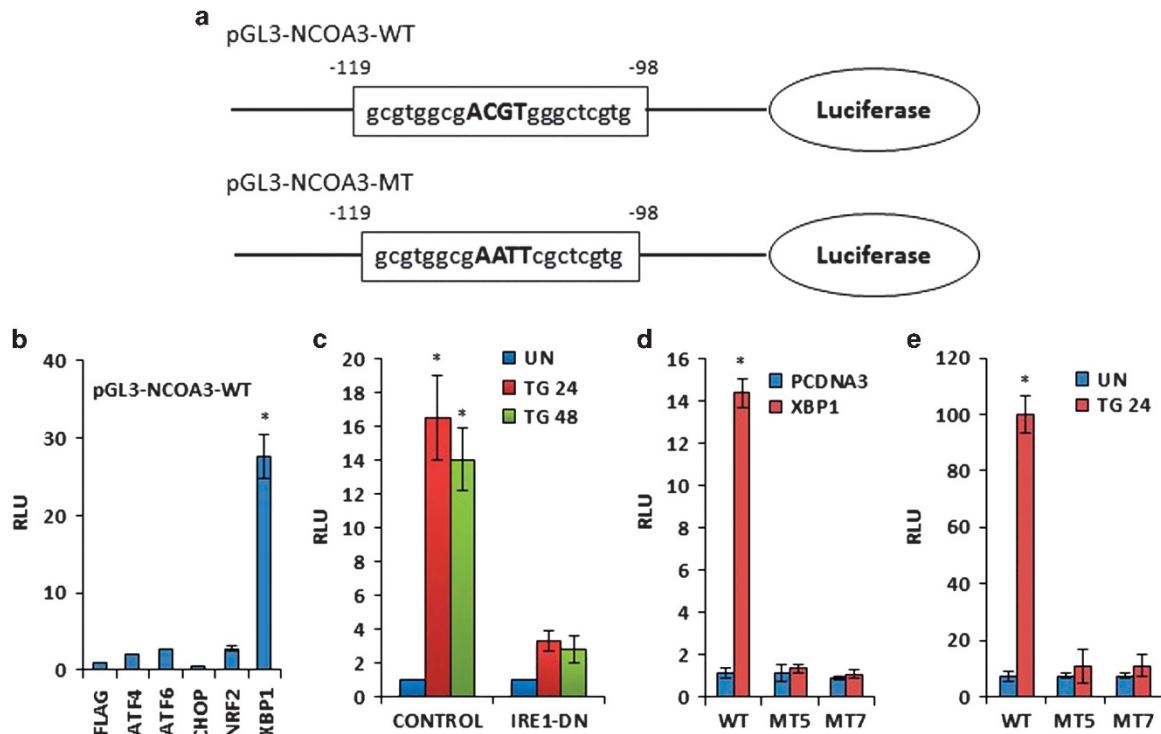


**Figure 3.** NCOA3 is a transcriptional target of XBP1. **(a)** Schematic representation of wild type (pGL3-NCOA3-WT) and XBP1-binding site mutant (pGL3-NCOA3-MT) human NCOA3 promoter reporter constructs. The nucleotide sequence of human NCOA3 promoter from position – 119 to – 98 relative to the transcription start site is shown. **(b)** 293T cells were transfected with pGL3-NCOA3-WT along with control (FLAG) or expression plasmid for indicated UPR transcription factors. Luciferase activity was measured 24 h after transfection and normalized luciferase activity (Firefly/Renilla) relative to control is shown. Error bars represent mean  $\pm$  s.d. from three independent experiments performed in duplicate. **(c)** 293T cells were transfected with pGL3-NCOA3-WT along with pcDNA3 (control) and pIRE1- $\Delta$ C (IRE1-DN). After 24 h of transfection, cells were either untreated (UN) or treated with (1.0  $\mu$ M) TG for indicated time points. Normalized luciferase activity (Firefly/Renilla) relative to untreated control is shown. Error bars represent mean  $\pm$  s.d. from three independent experiments performed in duplicate. **(d)** 293T cells were transfected with pGL3-NCOA3-WT or mutant pGL3-NCOA3-MT (MT5 and MT7) along with control (PCDNA3) or spliced XBP1 (XBP1) expression plasmid. Luciferase activity was measured 24 h post transfection and normalized luciferase activity (Firefly/Renilla) relative to control is shown. Error bars represent mean  $\pm$  s.d. from three independent experiments performed in duplicate. **(e)** 293T cells were transfected with pGL3-NCOA3-WT or mutant pGL3-NCOA3-MT (MT5 and MT7). Twenty-four hour post transfection, cells were either untreated (UN) or treated with (1.0  $\mu$ M) TG for indicated time points. Normalized luciferase activity (Firefly/Renilla) relative to untreated control is shown. Error bars represent mean  $\pm$  s.d. from three independent experiments performed in duplicate. \* $P$  < 0.05, two-tailed unpaired *t*-test compared with untreated cells.

reporter construct (pGL3-NCOA3-WT) containing this region was activated over 25-fold by cotransfection with spliced XBP1 in 293T cells (Figure 3b). To determine the role of endogenous XBP1 in regulating NCOA3 promoter, 293T cells were transfected with NCOA3 promoter-reporter plasmid along with dominant-negative IRE1 (IRE1 $\Delta$ C) and after 24 h they were treated with TG for 24 or 48 h. IRE1 $\Delta$ C mutant of IRE1 has been shown to attenuate EnR stress-induced production of spliced XBP1.<sup>23</sup> TG treatment resulted in up to 16-fold increase in NCOA3 promoter activity that was abolished by cotransfection of IRE1 $\Delta$ C mutant (Figure 3c). Mutation of the putative XBP1-binding site in NCOA3 promoter (pGL3-NCOA3-MT) completely abolished its transactivation by ectopic XBP1 (Figure 3d) and TG treatment (Figure 3e). These observations suggest that there is only one functional XBP1-responsive site in this region of NCOA3 promoter.

NCOA3 modulates optimal activation of the PERK-eIF2 $\alpha$ -ATF4 axis during UPR

Next we generated the clones of MCF7 cells expressing NCOA3 shRNA. For this purpose MCF7 cells were transduced with tetracycline-inducible lentivirus engineered to produce RFP and NCOA3 targeting shRNA upon addition of doxycycline and co-expression of the tetracycline regulatory protein, rtTA3. We observed significant knockdown of NCOA3 protein after the

addition of (500 ng/ml) doxycycline to MCF7-NCOA3-shRNA clone (Figure 4a). For subsequent experiments MCF7-NCOA3-shRNA cells were pre-treated with doxycycline (500 ng/ml) for 48 h to knockdown the expression of NCOA3. We observed that TG-induced increase in the expression of NCOA3 was attenuated by doxycycline in MCF7-NCOA3-shRNA clone (Figure 4b). Next, we tested whether NCOA3 modulated the activation of three branches of the UPR. For this purpose we used synthetic luciferase reporter constructs having ATF6- or XBP1-binding sites and CHOP-promoter reporter. The induction of the XBP1-binding site reporter and ATF6-binding site reporter in response to thapsigargin (TG) was not affected by knockdown of NCOA3 (Figure 4c). In contrast, the response of the CHOP-promoter reporter to TG was significantly decreased in the absence of NCOA3 (Figure 4c). PERK activation promotes both adaptive and apoptotic responses depending on the severity of the stress and context. In agreement with the proapoptotic role of the PERK pathway we observed that knockdown of NCOA3 provided resistance to EnR stress-mediated cell death (Figures 4d–e). Next we examined levels of UPR target genes to determine if NCOA3 modulated their expression. Levels of CHOP, HERP, GRP78 and XBP1-S were examined by quantitative reverse transcription-PCR (RT-PCR). No difference in UPR target genes expression was observed, with the notable exception of CHOP whose induction was consistently decreased in the presence of doxycycline (Figure 4f). PERK-eIF2 $\alpha$ -ATF4 branch of

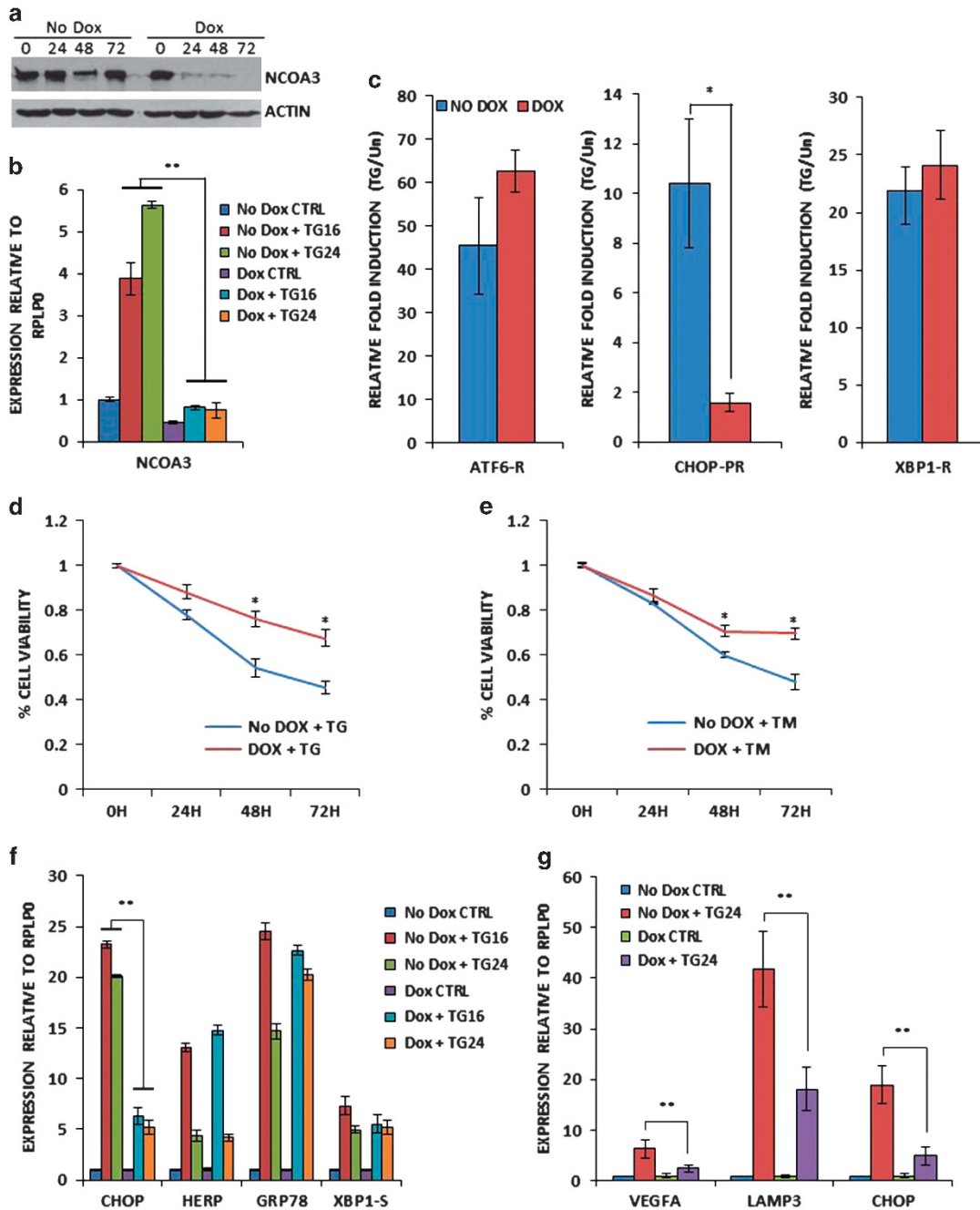


**Figure 4.** NCOA3 is required for ER stress-induced activation of the PERK-ATF4-CHOP axis. **(a)** pTRIPZshNCOA3-MCF7 cells were either untreated (No Dox) or treated (Dox) with (500 ng/ml) of doxycycline for indicated time points. Upper panel, equivalent amounts of cell lysates were resolved by sodium dodecyl sulphate-polyacrylamide gel electrophoresis and immunoblotting was performed using antibodies against NCOA3 and  $\beta$ -actin. **(b)** pTRIPZshNCOA3-MCF7 cells were either untreated (CTRL) or treated with (1.0  $\mu$ M) TG for indicated time points in the absence and presence of doxycycline. The expression level of NCOA3 was quantified by real-time RT-PCR, normalizing against RPLP0. Error bars represent mean  $\pm$  s.d. from three independent experiments performed in triplicate. **(c)** pTRIPZshNCOA3-MCF7 cells were transfected with the indicated UPR pathway reporter genes (ATF6-R, CHOP-PR, XBP1-R). Transfected cells were treated with TG (1.0  $\mu$ M) in the absence and presence of doxycycline for 24 h. Normalized luciferase activity (Firefly/Renilla) relative to untreated control is shown. Error bars represent mean  $\pm$  s.d. from three independent experiments performed in duplicate. **(d, e)** pTRIPZshNCOA3-MCF7 cells were untreated (CTRL) or treated with (1.0  $\mu$ M) TG and (1.0  $\mu$ g/ml) TM in the absence and presence of (500 ng/ml) of doxycycline for indicated time points. Line graphs show the absorbance in cells at the indicated time points after the treatment. Error bars represent mean  $\pm$  s.d. from three independent experiments performed in triplicate. **(f, g)** pTRIPZshNCOA3-MCF7 cells were either untreated (CTRL) or treated with (1.0  $\mu$ M) TG for indicated time points in the absence and presence of doxycycline. The expression level of CHOP, HERP, GRP78, XBP1-S, VEGFA and LAMP3 was quantified by real-time RT-PCR, normalizing against RPLP0. Error bars represent mean  $\pm$  s.d. from three independent experiments performed in triplicate. \* $P < 0.05$ , two-tailed unpaired  $t$ -test comparing TG-induced samples; \*\* $P < 0.05$ , two-tailed unpaired  $t$ -test comparing respective time points.

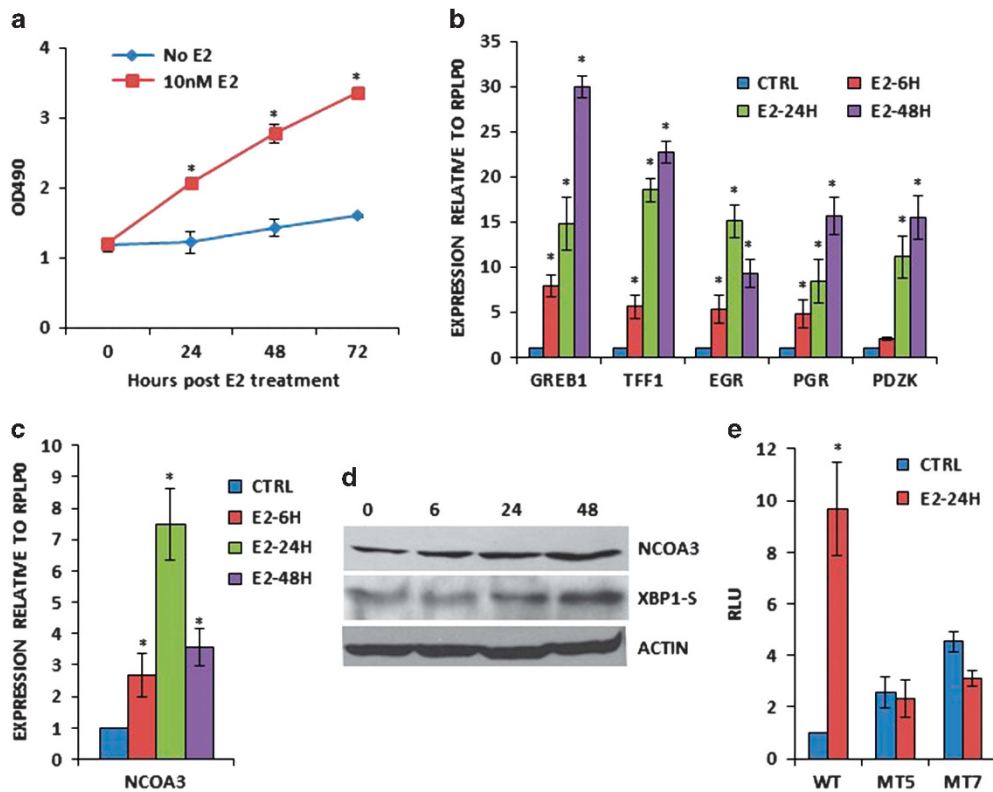


**Figure 5.** Induction of NCOA3 expression during oestrogen signalling. (a) MCF7 cells were synchronized before oestrogen treatment as described in the Materials and Methods section. After synchronization, cells were either untreated (No E2) or treated with (10 nM E2) oestrogen in 1% dextran-coated charcoal-stripped fetal bovine serum (DCC-FBS) supplemented medium. Line graphs show the absorbance in cells at the indicated time points after E2 treatment. Error bars represent mean  $\pm$  s.d. from three independent experiments performed in triplicate. (b, c) MCF7 cells were treated as in (a) and induction of E2-responsive genes (GREB1, TFF1, EGR, PGR and PDZK) and NCOA3 was quantified by real-time RT-PCR, normalizing against RPLP0. Error bars represent mean  $\pm$  s.d. from three independent experiments performed in triplicate. (d) MCF7 cells were treated as in (a), and western blotting of total protein was performed using antibodies against NCOA3, XBP1-S and  $\beta$ -actin. (e) MCF7 cells were transfected with pGL3-NCOA3-WT or mutant pGL3-NCOA3-MT (MT5 and MT7). Transfected cells were left either untreated (CTRL) or treated (E2-24H) with (10 nM) oestrogen. Normalized luciferase activity (Firefly/Renilla) relative to untreated control is shown. Error bars represent mean  $\pm$  s.d. from three independent experiments performed in duplicate. \* $P < 0.05$ , two-tailed unpaired *t*-test compared with untreated cells.

UPR has been shown to upregulate VEGFA and LAMP3 to induce angiogenesis and cell migration, respectively.<sup>24,25</sup> Indeed we observed that PERK inhibitor compromised the induction of VEGFA and LAMP3 during conditions of ER stress in MCF7 cells (Supplementary SF4). In agreement with its effect on induction of CHOP gene expression during UPR, knockdown of NCOA3 attenuated the TG-mediated induction of VEGFA and LAMP3 in MCF7 cells (Figure 4g). These results suggest that NCOA3 does not affect the ATF6 or IRE1-XBP1 axis but is required for the optimal activation of the PERK-eIF2 $\alpha$ -ATF4 pathway in response to EnR stress.

#### Oestrogen upregulates NCOA3 expression in IRE1-XBP1-dependent manner

Next we determined whether XBP1 regulates NCOA3 expression upon E2 stimulation. We first optimized the conditions for the E2-dependent growth and induction of bona fide E2-target genes in MCF7 cells. After synchronization for 72 h, MCF7 cells were treated with (10 nM) E2 in 1% dextran-coated charcoal-stripped fetal bovine serum supplemented medium. We observed a time-dependent growth of MCF7 cells (Figure 5a) and induction of (GREB1, TFF1, EGR, PGR and PDZK) bona fide E2-responsive genes (Figure 5b) under these conditions. We observed significant increase in NCOA3 mRNA and protein levels starting 6 h after the onset of E2 treatment and lasting for 48 h (Figures 5c and d).

Similar increase in the expression of NCOA3 following E2 stimulation was observed in T47D cells (Supplementary SF5). Next we investigated the role of IRE1-XBP1 axis in the regulation of the NCOA3 expression upon E2 signalling. We found that wild-type NCOA3 promoter reporter construct (pGL3-NCOA3-WT) was upregulated 8–12 fold by E2 treatment (Figure 5e). This upregulation was completely abrogated in XBP1-binding site mutant NCOA3 promoter reporter construct (Figure 5e). Next we determined the effect of IRE1 inhibitors (4 $\mu$ 8C and STF083010) on E2-mediated induction of NCOA3 expression. We found that 4 $\mu$ 8C and STF083010 efficiently attenuated the E2-stimulated growth and increase in the expression of XBP1-S, GREB1 and NCOA3 (Figures 6a and b). These results suggest that induction of NCOA3 during E2 stimulation is dependent on RNase activity of IRE1. Next we used the control (MCF7-PLKO) and XBP1 knockdown subclones (MCF7-XKD) of MCF7 cells to determine the role of XBP1 in the regulation of the NCOA3 expression upon E2 signalling. We found that knockdown of XBP1 compromised E2-stimulated growth as well as expression of XBP1-S, GREB1 and NCOA3 (Figures 6c and d). Collectively, these results suggest that induction of NCOA3 during E2 stimulation is dependent on the IRE1-XBP1 axis.

#### NCOA3 is required for E2-mediated upregulation of XBP1

Next we determined the role of upregulated NCOA3 in oestrogen signalling and XBP1-mediated antioestrogen resistance. After

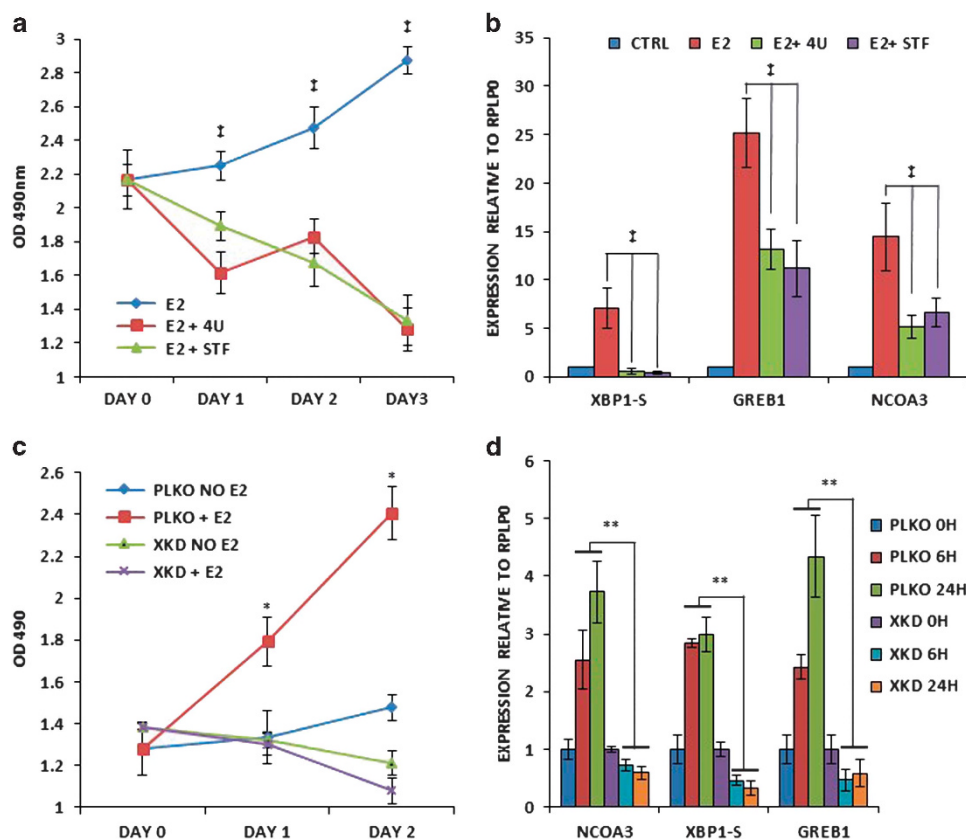


**Figure 6.** IRE1–XBP1 signalling is required for E2-mediated growth and expression of NCOA3. **(a)** MCF7 cells were treated with (10 nM) oestrogen in the absence and presence of IRE1 inhibitors, (10 μM) 4μ8C (4 U) and (100 μM) STF083010 (STF) for indicated time points. Line graphs show the absorbance in cells at the indicated time points after the treatment with IRE1 inhibitors. **(b)** MCF7 cells were treated as in **(a)**, for 24 h. Expression of XBP1-S, GREB1 and NCOA3 was quantified by real-time RT–PCR, normalizing against RPLP0. Error bars represent mean ± s.d. from three independent experiments performed in triplicate. **(c)** MCF7-control (PKLO) and MCF7-XBP1 knockdown (XKD) cells were synchronized as described in the Materials and methods section. After synchronization, cells were treated with (10 nM) E2 in 1% dextran-coated charcoal-stripped fetal bovine serum (DCC-FBS) supplemented medium. Line graphs show the absorbance in cells at the indicated time points after the E2 treatment. Error bars represent mean ± s.d. from three independent experiments performed in triplicate. **(d)** MCF7-control (PKLO) and MCF7-XBP1 knockdown (XKD) cells were treated as in **(c)**, for indicated time points. Expression of spliced XBP1 (XBP1-S), total XBP1 (XBP1-F), GREB1 and NCOA3 was quantified by real-time RT–PCR, normalizing against RPLP0. Error bars represent mean ± s.d. from three independent experiments performed in triplicate. \**P* < 0.05, two-tailed unpaired *t*-test compared with untreated cells; †*P* < 0.05 for one-way ANOVA; \*\**P* < 0.05, two-tailed unpaired *t*-test comparing respective time points.

synchronization for 72 h, MCF7-NCOA3-shRNA cells were treated with (10 nM) E2 in the absence and presence of doxycycline (500 ng/ml). We observed that knockdown of NCOA3 expression attenuated the E2-stimulated growth as well as expression of XBP1-S, GREB1 and NCOA3 (Figures 7a and b). To evaluate the role of NCOA3 in XBP1-mediated resistance to antioestrogens MCF7-NCOA3-shRNA cells were transfected with XBP1-S expressing plasmid. Fulvestrant, a selective oestrogen receptor downregulator is a pure competitive antagonist of oestrogen receptor alpha.<sup>26</sup> We found that ectopic XBP1-S provided the resistance to fulvestrant and knockdown of NCOA3 abrogated the resistance provided by XBP1-S (Figure 7c). In addition, NCOA3 knockdown cells showed increased sensitivity to fulvestrant, further underscoring a role for NCOA3 in antioestrogen resistance.

Higher levels of NCOA3 mRNA in breast tumours are associated with a poor prognosis

Breast tumour specimens (*n* = 60) were retrieved from patients undergoing primary curative resection at University Hospital Galway, Ireland. Matched tumour-associated normal breast tissue was also obtained from a subset (*n* = 10) of these patients where possible. Clinical and pathological data related to the samples are

presented in Supplementary SF6. The total RNA from breast tumour (*n* = 60) and tumour-associated normal breast tissue (*n* = 10) specimens was used to quantify levels of NCOA3 gene expression. NCOA3 levels were observed to be dysregulated in different subtypes of breast cancer samples than in normal breast tissue (Figure 8a). An increase in tumour stage (log-rank; *P* = 0.009) and NCOA3 expression was associated with shorter overall survival (log-rank; *P* = 0.043). Prognostic significance of these parameters remained after multivariate analysis. No other statistically significant associations between high NCOA3 expression and clinicopathological variables (age at diagnosis, macroscopic tumour size and lymph node status), or biomarker expression, were found. Associations between NCOA3 expression and outcome were examined by dichotomizing the NCOA3 expression as low and high at the median. We observed that in the patient samples, higher NCOA3 expression was associated with reduced overall survival (Figure 8b) and disease-free survival (Figure 8c) as compared with low NCOA3 expression. Furthermore, higher XBP1 mRNA in breast tumour samples correlated with a higher NCOA3 mRNA level (Figure 8d). Overall, these results suggest that higher XBP1 is associated with increased NCOA3 gene expression in human breast cancer tumours and poor outcome in human patients.

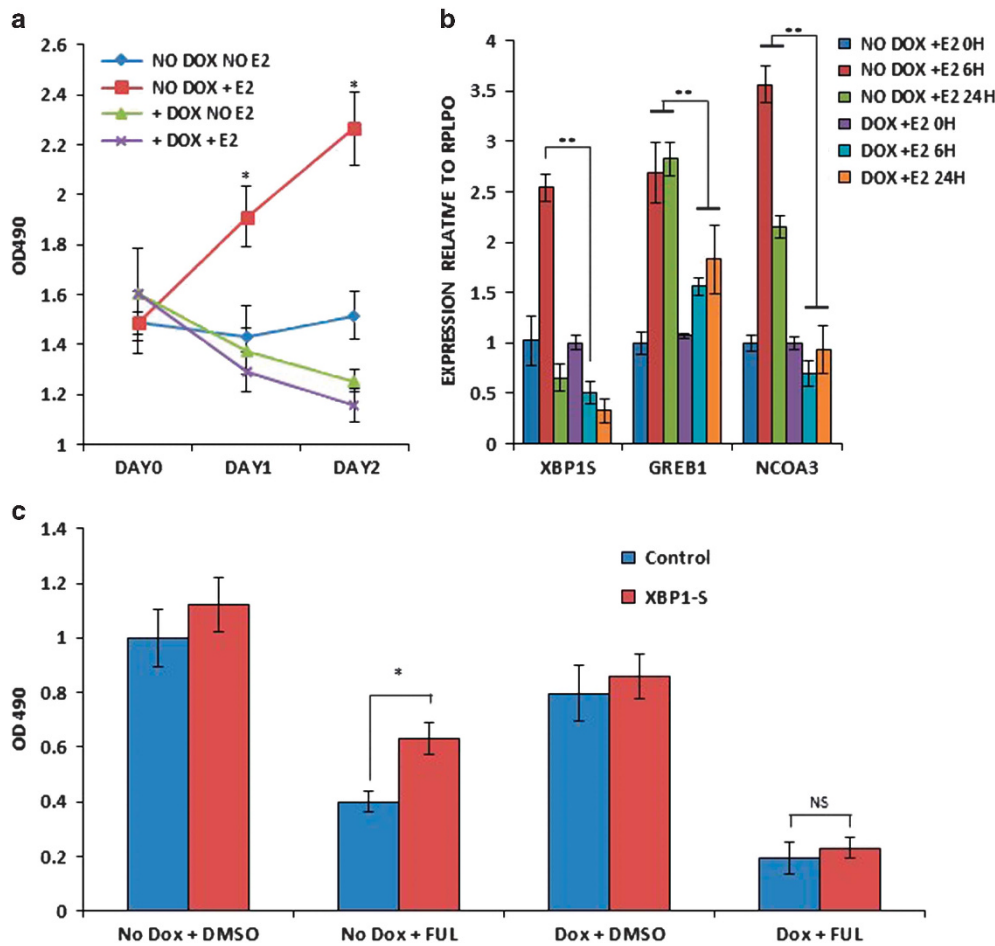


**Figure 7.** NCOA3 regulates induction of XBP1 upon oestrogen signalling and is required for XBP1-mediated antioestrogen resistance. (a) pTRIPZshNCOA3-MCF7 cells were treated with (10 nM) oestrogen in the absence and presence of (500 ng/ml) of doxycycline for indicated time points. Line graphs show the absorbance in cells at the indicated time points after the E2 treatment. Error bars represent mean  $\pm$  s.d. from three independent experiments performed in triplicate. (b) pTRIPZshNCOA3-MCF7 cells were treated with (10 nM) oestrogen in the absence and presence of (500 ng/ml) of doxycycline for indicated time points. The expression level of spliced XBP1 (XBP1-S), GREB1 and NCOA3 was quantified by real-time RT-PCR, normalizing against RPLP0. Error bars represent mean  $\pm$  s.d. from three independent experiments performed in triplicate. (c) pTRIPZshNCOA3-MCF7 cells transfected with control or XBP1-S plasmid and were treated with (1  $\mu$ M) fulvestrant in the absence and presence of (500 ng/ml) of doxycycline for 48 h. MTS cell proliferation assay was performed to assess the changes in cell density. \* $P$  < 0.05, two-tailed unpaired *t*-test compared with untreated cells; \*\* $P$  < 0.05, two-tailed unpaired *t*-test comparing respective time points. NS, not significant.

## DISCUSSION

Spliced XBP1 (XBP1-S), a member of the activated transcription factor (ATF) family of transcription factors, is a key component of the UPR. XBP1-S plays a crucial role in development of highly secretory cells, such as exocrine pancreas, Paneth cells and antibody-producing plasma cells.<sup>27</sup> Several gene expression profiling studies have revealed that XBP1-S induces the expression of a core group of genes involved in constitutive maintenance of endoplasmic reticulum function in almost all cell types.<sup>28</sup> In addition, there is a unique subset of XBP1-regulated genes that vary in the context of specific stimuli and cell types, such as Wolfram syndrome 1 (*WFS1*) in neuronal cells,<sup>29</sup> basic helix-loop-helix family, member a15 (*BHLHA15*) in myoblasts.<sup>27</sup> Recently Chen *et al.*<sup>30</sup> have shown that XBP1 plays an important role in progression of triple negative breast cancer by regulating the HIF1 $\alpha$  transcriptional programme. In this report we show that XBP1-S plays an important role in increased expression of NCOA3 during conditions of UPR and oestrogen stimulation (Figure 9). NCOA3 has been shown to play an important role in the tumorigenesis and progression of hormone-dependent as well as hormone-independent cancers.<sup>11,13</sup> The expression of NCOA3 is

elevated in human cancers in the absence of gene amplification and relatively little is known about mechanisms of NCOA3 overexpression.<sup>18</sup> The stressful conditions in the tumour micro-environment, including low oxygen supply, nutrient deprivation and pH changes, activate a range of cellular stress-response pathways.<sup>31</sup> Cellular adaptation to stress in tumour microenvironment occurs through multiple mechanisms, including activation of the UPR.<sup>1</sup> Our results showing the increased expression of NCOA3 during conditions of UPR (Figures 1–3) provide a mechanism for overexpression of NCOA3 in human cancers.

Nuclear receptor coactivators (NCOAs) are associated with a diverse array of human diseases such as systemic metabolite homeostasis, inflammation, energy regulation and several types of human cancer.<sup>32</sup> An important question is how the expression/activity of NCOAs is regulated by diverse metabolic disruptions and stress responses. Chronic EnR stress and defects in UPR signalling are emerging as key contributors to a growing list of human diseases, including immune disorders, cardiovascular diseases, diabetes, neurodegeneration and cancer.<sup>31,33</sup> In light of our results showing IRE1–XBP1-dependent upregulation of NCOA3 during UPR and ample overlap of human diseases where a role for NCOAs and UPR has been implicated, we posit that UPR-mediated



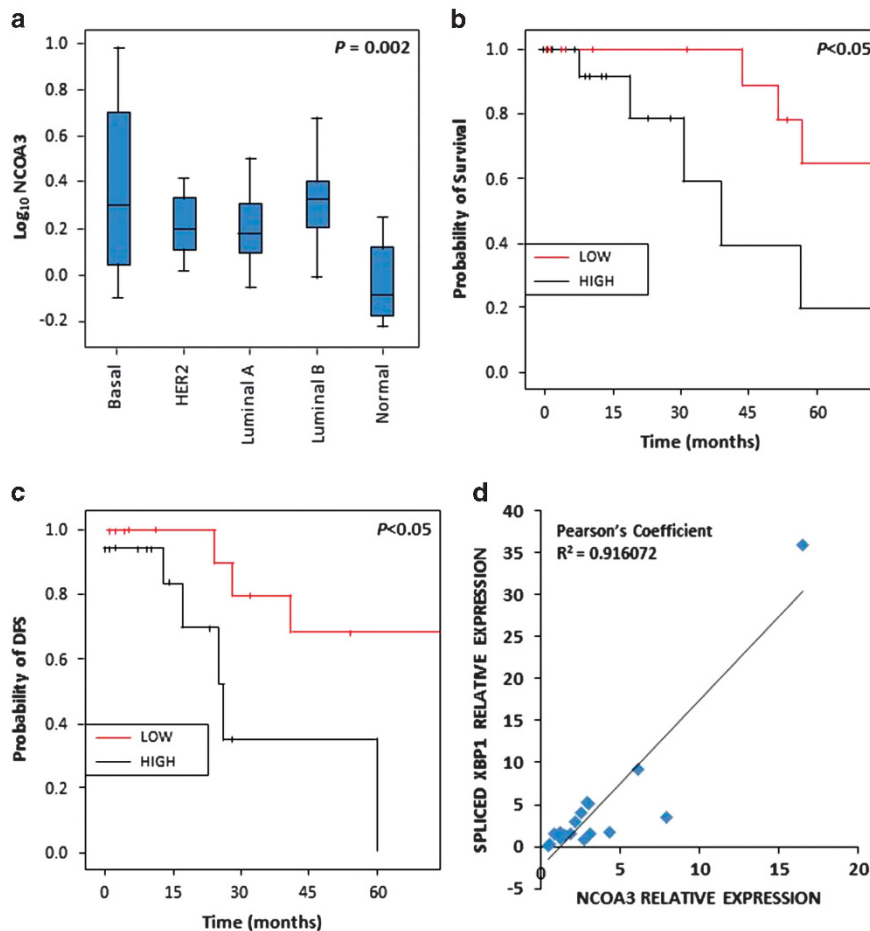


**Figure 8.** NCOA3 expression is higher in XBP1-expressing breast cancer tumours. **(a)** Significant differences in relative expression of NCOA3 transcripts in breast tumour subtypes ( $n = 60$ ) and tumour-associated normal ( $n = 10$ ) breast tissue. Box-plot shows the expression of NCOA3 in breast cancer subtypes (Luminal A ( $n = 18$ ); Luminal B ( $n = 19$ ); Basal-like ( $n = 15$ ); HER2 overexpressing ( $n = 80$ )) and tumour-associated normal breast tissue (ANOVA  $P < 0.002$ ). **(b, c)** Kaplan–Meier survival analysis and log-rank test were used to assess the statistical significance of survival difference. Kaplan–Meier curves for overall survival **(b)** and disease-free survival **(c)** in invasive breast cancer categorized according to NCOA3 expression. **(d)** Correlation between the expression of spliced XBP1 and NCOA3 in the breast cancer samples. The expression level of spliced XBP1 and NCOA3 was quantified by real-time RT–PCR, normalizing against RPLP0. The square of the Pearson correlation coefficient is 0.91.

induction of NCOA3 may play a role in coordination of NCOA3 activity in accordance with the metabolic demand.

Our results uncover a novel non-NR role for NCOA3 in the UPR signalling, where NCOA3 plays an important role in optimal activation of the PERK–eIF2 $\alpha$ –ATF4 pathway, but has no significant effect on IRE1–XBP1 or ATF6 branches of UPR (Figure 4). As PERK signalling mediates both adaptive and apoptotic responses depending on the intensity and duration of the stress, it may promote, as well as suppress, malignant transformation depending on the context.<sup>34,35</sup> Indeed we observed that knockdown of NCOA3 abrogated PERK signalling and provided resistance to EnR stress-mediated cell death (Figure 4). Loss of NCOA3 has been shown to accelerate polyoma middle-T antigen-induced mammary tumorigenesis and malignant B-cell lymphomas in mice.<sup>36,37</sup> However, further investigation is required to evaluate whether loss of NCOA3 contributes to cancer progression by inhibiting EnR stress-induced apoptosis in tumour microenvironment. The PERK–ATF4 arm directly upregulates vascular endothelial growth factor A (VEGFA) and Lysosomal-Associated Membrane Protein 3 (LAMP3), thereby regulating tumour vascularity and invasion.<sup>25,38</sup> In line, tumours derived from K-Ras-transformed embryonic fibroblasts derived from PERK knockout mice show severely

compromised tumour vascularization<sup>39</sup> and PERK-deficient mice have reduced growth of  $\beta$ -cell insulinoma tumours as a result of compromised tumour vascularization.<sup>40</sup> Indeed, the PERK inhibitor and knockdown of NCOA3 both attenuated the UPR-mediated increase in the expression of VEGF and LAMP3 (Figure 4 and Supplementary SF3). Further epithelial to mesenchymal transition activates PERK–eIF2 $\alpha$  signalling, which is required for invasion and metastasis of primary tumour.<sup>41</sup> Taken together our results suggest a role for NCOA3 in PERK-dependent effects on malignant transformation.

Our results show that XBP1-S regulates the expression of NCOA3 upon oestrogen stimulation via the XBP1-binding sites in the promoter of NCOA3 (Figures 5 and 6). Further we show that NCOA3 is required for induction of XBP1-S upon E2 stimulation (Figure 7) but not during the conditions of EnR stress (Figure 4). During conditions of E2 stimulation, the oestrogen receptor is recruited to the enhancer region of XBP1 gene leading to induction of XBP1 mRNA, which is then spliced by IRE1 to produce XBP1-S.<sup>5</sup> However ATF6 induces the expression of XBP1 mRNA during UPR, which is then spliced by IRE1 to produce XBP1-S.<sup>42</sup> In agreement with these observations, we found that loss of NCOA3 had no effect on transcriptional activity of ATF6 (Figure 4c)

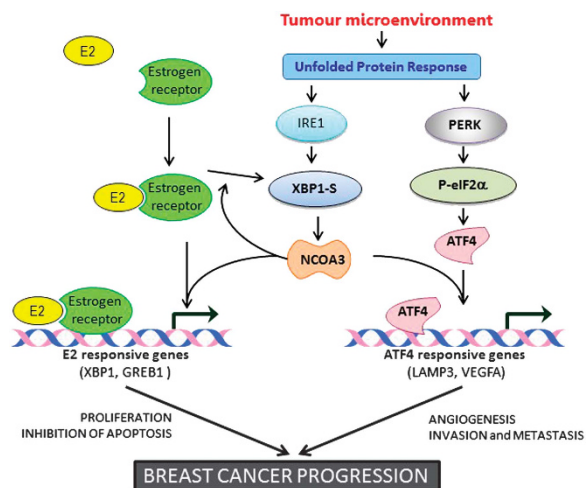


**Figure 9.** Graphical abstract. Stressful conditions of the tumour microenvironment activate an adaptive mechanism called the unfolded protein response (UPR). X-box binding protein-1 (XBP1) is a critical transcriptional activator that is induced by the UPR. In oestrogen receptor-positive (ER+) breast cancer cells XBP1 is rapidly induced in response to E2 stimulation. In luminal breast cancers oestrogen signalling and UPR induce the expression of XBP1s. Here we show that XBP1s upregulate the transcriptional activation of NCOA3 during oestrogen signalling and UPR. NCOA3 is required for the induction of oestrogen-responsive and PERK–ATF4-responsive genes. Our results suggest that XBP1s regulates growth and proliferation of ER-positive breast cancer cells, in part, by transcriptional activation of NCOA3.

but compromised the induction of E2-responsive genes (Figure 7b). We further show that NCOA3 is required for E2-dependent proliferation and induction of XBP1, thereby generating a feed forward autoregulatory loop (Figure 7). These results suggest that in cells with hyperactive XBP1-S, such as the case encountered in stressful conditions of tumour microenvironment, there is a positive feedback regulatory loop consisting of XBP1-S and NCOA3 to maintain high levels of NCOA3 and XBP1-S in ER-positive breast cancer. Indeed, we observed very good correlation between the transcript levels of NCOA3 and XBP1-S in breast cancer patient samples (Figure 8). Overexpression of XBP1-S can confer oestrogen-independent growth and resistance to anti-hormonal therapy.<sup>3</sup> Further XBP1-S is overexpressed in anti-oestrogen-resistant breast cancer cells and increased expression of XBP1-S is associated with poor clinical outcome.<sup>43</sup> Our results show that NCOA3 is required for XBP1-S mediated resistance to anti-oestrogens (Figure 7). XBP1 has been shown to regulate NF-κB activity, which plays an important role in XBP1-mediated effects on anti-oestrogen responsiveness.<sup>44</sup> NCOA3 interacts with I kappa B kinase (IKK) and is phosphorylated by the IKK complex.<sup>45</sup> Further phosphorylated NCOA3 potentiates NF-κB-mediated gene expression.<sup>45</sup> Thus activation of NCOA3 and NF-κB by XBP1 can act in a concerted manner to regulate anti-oestrogen responsiveness. Taken together our findings reveal a key function for the IRE1–XBP1–NCOA3 axis in luminal/ER-positive breast cancer and indicate that targeting this pathway may offer alternative treatment strategies for anti-oestrogen-resistant breast cancer.

## MATERIALS AND METHODS

### Cell culture and treatments

MCF7, T47D and MDA-MB231 cells were purchased from ECACC (Salisbury, UK). HEK 293T cells were from Indiana University National Gene Vector Biorepository (Indianapolis, IN, USA). Cells maintained in Dulbecco's modified medium supplemented with 10% fetal calf serum, 100 U/ml

penicillin and 100 mg/ml streptomycin at 37 °C with 5% CO<sub>2</sub>. To induce ER stress, cells were treated with TM or TG at the indicated concentrations for the indicated time. TG (Cat # 1138), TM (Cat # 3516), ICI 182,780 (Cat # 1047) were from Tocris Bioscience (Abingdon, UK). Estradiol (Cat# 1006315) was from Cayman Chemical (Ann Arbor, MI, USA). To inhibit IRE1 endoribonuclease activity, cells were treated with IRE1 inhibitor (4μ8C) (Cat # 412512; Merck Millipore Ltd, Cork, Ireland) and STF083010 (Cat# 412510; Merck Millipore Ltd). To inhibit PERK activity cells were treated with GSK2606414 (Cat # 516535; Merck Millipore Ltd).

### Oestrogen stimulated growth

Parental MCF7 cells or subclones (MCF-PLKO, MCF7-XKD and pTRIPZshNCOA3-MCF7) were synchronized before oestrogen treatment by incubation for 72 h in the phenol red-free medium supplemented with 1% dextran-coated charcoal-stripped fetal bovine serum. After synchronization, cells were treated with 10 nM E2 in 1% dextran-coated charcoal-stripped fetal bovine serum supplemented medium. Cultures were further incubated at 37 °C after which cells were assayed with 3-(4,5-dimethylthiazol-2-yl)-5-(3-carboxymethoxyphenyl)-2-(4-sulfophenyl)-2H-tetrazolium (MTS) cell proliferation assay at time intervals 1–5 days as indicated. Measurements were made in accordance with the manufacturer's instructions (Promega Corp., Madison, WI, USA).

### Plasmid constructs

The expression vector for pBMN-I-GFP, pBMN-hATF6(373)-I-GFP encoding aa 1–373 of human ATF6α and pBMN-hXBP1(S)-I-GFP encoding full-length human XBP1 generated by UPR-mediated splicing were a kind gift from Dr Joseph Brewer (University of South Alabama, Mobile, AL, USA). The expression vector for FLAG-tagged ATF4 (pRK-ATF4) was a gift from Yihong Ye (Addgene plasmid # 26114; Cambridge, MA, USA); FLAG-tagged NRF2 (NC16 pCDNA3.1-FLAG-NRF2) was a gift from Randall Moon (Addgene plasmid # 36971). The expression vector for FLAG-tagged CHOP (pcDNA3-FLAG-CHOP) was a kind gift from Dr Wolfgang Dubiel (Humboldt University, Germany). The pGL3-ACTR-1.6 kb construct was a kind gift from Dr Hongwu Chen (University of California, Davis, CA, USA) and contains a genomic DNA fragment (1.6 kb, *HindIII–NcoI*) containing the first exon of NCOA3 into vector pGL3-basic. The ATF6, PERK and IRE1–XBP1 pathway reporters has been described previously.<sup>46</sup>

### Generation of stable cell lines

The control and XBP1-targeting shRNA plasmid (TRCN0000019805) was from Sigma (Wicklow, Ireland). The tetracycline-inducible pTRIPZ NCOA3 shRNA plasmid (V2THS\_261936) with targeting sequence 5'-GTCAGATAAGCAGGAGGTA-3' was from Thermo Scientific (St Leon-Rot, Germany). Lentivirus was generated by transfecting lentiviral plasmids along with packaging plasmids in 293T cells using jetPEI transfection reagent (Polyplus transfection, VWR International Ltd, Dublin, Ireland) according to the manufacturer's instructions. MCF7 cells were then transduced with the shRNA lentivirus and selection for shRNA-positive cells was performed with 2 μg/ml puromycin for 7 days.

### RNA extraction, RT-PCR and real-time RT-PCR

Total RNA was isolated using Trizol (Fisher Scientific Ireland Ltd, Dublin, Ireland) according to the manufacturer's instructions. RT was carried out with 2 μg RNA and random primers (Promega) using ImProm-II Reverse Transcription System (Promega). The real-time PCR method to determine the induction of UPR target genes has been described previously.<sup>47</sup>

### Luciferase reporter assays

The wild-type NCOA3 human promoter reporter construct (pGL3-ACTR-1.6 kb) was used to generate XBP1-binding site mutant construct. Point mutations in pGL3-ACTR-1.6 kb were performed using the QuikChange site-directed mutagenesis method. The following forward primers were used to produce point mutations in XBP1-binding site of pGL3-NCOA3-WT construct (NCOA3-MUT-Forward) 5'-CGGAGGGCGTGGCGAATTCGGCTCGT GCGGCCG-3', and (NCOA3-MUT-Reverse) 5'-CGGCCGCTCGAGCCGAATTC GCCACGCCCTCCG-3'. The generated mutants were verified by restriction enzyme digestion because the mutations introduced an *EcoRI* site in the pGL3-NCOA3-MT plasmid and confirmed by sequencing. In promoter assays, 293T cells were grown in a six-well plate and transfected with (1.0 μg) pGL3-NCOA3-WT or pGL3-NCOA3-MT reporter constructs in

combination with (100 ng) Renilla luciferase vector as an internal control. Twenty-four hours post transfection cells were treated with TG or TM for 24 h. Firefly luciferase and Renilla luciferase activities were measured 48 h after transfection using Lucetta Luminometer (Lonza, Castelford, UK) and then normalized for Renilla luciferase activity.

### Western blotting

Western blotting procedures has been described previously.<sup>48</sup> The primary antibodies used were ATF6 (Abcam, Cambridge, UK, Cat# ab122897), spliced XBP1 (Biolegend, London, UK, Cat# 619502), PERK (Cell signalling, Cat# C33E10), GRP78 (Fisher Scientific Ireland Ltd, Cat# PA1-014A), phospho-eIF2 $\alpha$  (Cell signalling, Cat# 9721), total eIF2 $\alpha$  (Cell signalling, Cat# 9722) and or  $\beta$ -actin (Sigma, Cat# A-5060) overnight at 4 °C. The membrane was washed three times with PBS-0.05% Tween and further incubated in appropriate horseradish peroxidase-conjugated secondary antibody (Fisher Scientific Ireland Ltd) for 90 min. Signals were detected using Western Lightening Plus ECL (Perkin Elmer, Dublin, Ireland).

### Patients and tumour samples

Breast tumour specimens ( $n=60$ ) were retrieved from patients undergoing primary curative resection at University Hospital Galway, Ireland. Matched tumour-associated normal breast tissue was also obtained from a subset ( $n=10$ ) of these patients where possible. Following excision, tissue samples were immediately snap-frozen in liquid nitrogen and stored at  $-80$  °C until RNA extraction. Prior written and informed consent was obtained from each patient and the study was approved by the ethics review board of University Hospital Galway. Clinical and pathological data related to the samples are presented in Supplementary SF6.

### RNA extraction and NCOA3 expression analysis

Tissue samples (50–100 mg) were homogenized using a hand-held homogenizer (Polytron PT1600E; Kinematica AG, Littau-Luzern, Switzerland) in 1–2 ml of Trizol. RNA was extracted and levels of NCOA3 gene expression were quantified by quantitative RT-PCR using TaqMan assays. Relationships between gene expression levels and clinic-pathological parameters, intrinsic subtype and clinical outcomes were analysed using Pearson  $s$  correlation coefficient, Student's  $t$ -test, ANOVA, Kaplan–Meier survival curves and Cox proportional hazards model with SPSS software.  $P < 0.05$  was considered significant.

### Statistical analysis

The data are expressed as mean  $\pm$  s.d. for three independent experiments. Differences between the treatment groups were assessed using two-tailed paired Student's  $t$ -tests. The values with a  $P < 0.05$  were considered statistically significant.

### CONFLICT OF INTEREST

The authors declare no conflict of interest.

### ACKNOWLEDGEMENTS

This publication has emanated from research conducted with the financial support of Health Research Board (grant number HRA\_HSR/2010/24) and Breast Cancer campaign (grant number 2011PR26).

### AUTHOR CONTRIBUTIONS

The authors have made the following contributions: conceived and designed the experiments: AG, GC and SG; performed the experiments: AG, MMH, NM and SG; analysed the data: AG, MMH and SG; and contributed reagents/materials/analysis tools: NM and MK. The text and figures were prepared by AG, NM and SG. All authors reviewed the manuscript.

### REFERENCES

- Wang M, Kaufman RJ. The impact of the endoplasmic reticulum protein-folding environment on cancer development. *Nat Rev Cancer* 2014; **14**: 581–597.
- Read DE, Gupta A, Cawley K, Gupta S. Regulation of ER stress responses by microRNAs. In: Agostinis P, Afshin S (eds). *Endoplasmic Reticulum Stress in Health and Disease*. Springer: Netherlands, 2012, pp 143–161.
- Musgrove EA, Sutherland RL. Biological determinants of endocrine resistance in breast cancer. *Nat Rev Cancer* 2009; **9**: 631–643.
- Cancer Genome Atlas Network. Comprehensive molecular portraits of human breast tumours. *Nature* 2012; **490**: 61–70.
- Carroll JS, Liu XS, Brodsky AS, Li W, Meyer CA, Szary AJ et al. Chromosome-wide mapping of estrogen receptor binding reveals long-range regulation requiring the forkhead protein FoxA1. *Cell* 2005; **122**: 33–43.
- Sengupta S, Sharma CG, Jordan VC. Estrogen regulation of X-box binding protein-1 and its role in estrogen induced growth of breast and endometrial cancer cells. *Horm Mol Biol Clin Investig* 2010; **2**: 235–243.
- Ding L, Yan J, Zhu J, Zhong H, Lu Q, Wang Z et al. Ligand-independent activation of estrogen receptor alpha by XBP-1. *Nucleic Acids Res* 2003; **31**: 5266–5274.
- Gomez BP, Riggins RB, Shajahan AN, Klimach U, Wang A, Crawford AC et al. Human X-box binding protein-1 confers both estrogen independence and antiestrogen resistance in breast cancer cell lines. *FASEB J* 2007; **21**: 4013–4027.
- Romero-Ramirez L, Cao H, Nelson D, Hammond E, Lee AH, Yoshida H et al. XBP1 is essential for survival under hypoxic conditions and is required for tumor growth. *Cancer Res* 2004; **64**: 5943–5947.
- Clarke R, Cook KL. Unfolding the role of stress response signaling in endocrine resistant breast cancers. *Front Oncol* 2015; **5**: 140.
- Lydon JP, O'Malley BW. Minireview: steroid receptor coactivator-3: a multifarious coregulator in mammary gland metastasis. *Endocrinology* 2011; **152**: 19–25.
- Torres-Arzuayus MI, Font de Mora J, Yuan J, Vazquez F, Bronson R, Rue M et al. High tumor incidence and activation of the PI3K/AKT pathway in transgenic mice define AIB1 as an oncogene. *Cancer Cell* 2004; **6**: 263–274.
- Xu J, Wu RC, O'Malley BW. Normal and cancer-related functions of the p160 steroid receptor co-activator (SRC) family. *Nat Rev Cancer* 2009; **9**: 615–630.
- Xu J, Liao L, Ning G, Yoshida-Komiya H, Deng C, O'Malley BW. The steroid receptor coactivator SRC-3 (p/CIP/RAC3/AIB1/ACTR/TRAM-1) is required for normal growth, puberty, female reproductive function, and mammary gland development. *Proc Natl Acad Sci USA* 2000; **97**: 6379–6384.
- Johnson AB, O'Malley BW. Steroid receptor coactivators 1, 2, and 3: critical regulators of nuclear receptor activity and steroid receptor modulator (SRM)-based cancer therapy. *Mol Cell Endocrinol* 2012; **348**: 430–439.
- Zhao C, Yasui K, Lee CJ, Kurioka H, Hosokawa Y, Oka T et al. Elevated expression levels of NCOA3, TOP1, and TFAP2C in breast tumors as predictors of poor prognosis. *Cancer* 2003; **98**: 18–23.
- Murphy LC, Simon SL, Parkes A, Leygue E, Dotzlaw H, Snell L et al. Altered expression of estrogen receptor coregulators during human breast tumorigenesis. *Cancer Res* 2000; **60**: 6266–6271.
- Anzick SL, Kononen J, Walker RL, Azorsa DO, Tanner MM, Guan XY et al. AIB1, a steroid receptor coactivator amplified in breast and ovarian cancer. *Science* 1997; **277**: 965–968.
- Cawley K, Deegan S, Samali A, Gupta S. Assays for detecting the unfolded protein response. *Methods Enzymol* 2011; **490**: 31–51.
- Axten JM, Medina JR, Feng Y, Shu A, Romeril SP, Grant SW et al. Discovery of 7-methyl-5-(1-[[3-(trifluoromethyl)phenyl]acetyl]-2,3-dihydro-1H-indol-5-yl]-7H-pyrrolo[2,3-d]pyrimidin-4-amine (GSK2606414), a potent and selective first-in-class inhibitor of protein kinase R (PKR)-like endoplasmic reticulum kinase (PERK). *J Med Chem* 2012; **55**: 7193–7207.
- Cross BC, Bond PJ, Sadowski PG, Jha BK, Zak J, Goodman JM et al. The molecular basis for selective inhibition of unconventional mRNA splicing by an IRE1-binding small molecule. *Proc Natl Acad Sci USA* 2012; **109**: E869–E878.
- Papandreou I, Denko NC, Olson M, Van Melckebeke H, Lust S, Tam A et al. Identification of an Ire1 $\alpha$  endonuclease specific inhibitor with cytotoxic activity against human multiple myeloma. *Blood* 2011; **117**: 1311–1314.
- Samali A, Fitzgerald U, Deegan S, Gupta S. Methods for monitoring endoplasmic reticulum stress and the unfolded protein response. *Int J Cell Biol* 2010; **2010**: 830307.
- Nagelkerke A, Bussink J, Mujcic H, Wouters BG, Lehmann S, Sweep FC et al. Hypoxia stimulates migration of breast cancer cells via the PERK/ATF4/LAMP3-arm of the unfolded protein response. *Breast Cancer Res* 2013; **15**: R2.
- Mujcic H, Nagelkerke A, Rouschop KM, Chung S, Chaudary N, Span PN et al. Hypoxic activation of the PERK/elf2 $\alpha$  arm of the unfolded protein response promotes metastasis through induction of LAMP3. *Clin Cancer Res* 2013; **19**: 6126–6137.

- 26 Wijayaratne AL, McDonnell DP. The human estrogen receptor-alpha is a ubiquitinated protein whose stability is affected differentially by agonists, antagonists, and selective estrogen receptor modulators. *J Biol Chem* 2001; **276**: 35684–35692.
- 27 Acosta-Alvear D, Zhou Y, Blais A, Tsikitis M, Lents NH, Arias C *et al*. XBP1 controls diverse cell type- and condition-specific transcriptional regulatory networks. *Mol Cell* 2007; **27**: 53–66.
- 28 Hetz C, Martinon F, Rodriguez D, Glimcher LH. The unfolded protein response: integrating stress signals through the stress sensor Ire1 alpha. *Physiol Rev* 2011; **91**: 1219–1243.
- 29 Kakiuchi C, Ishiwata M, Hayashi A, Kato T. XBP1 induces WFS1 through an endoplasmic reticulum stress response element-like motif in SH-SY5Y cells. *J Neurochem* 2006; **97**: 545–555.
- 30 Chen X, Iliopoulos D, Zhang Q, Tang Q, Greenblatt MB, Hatziaepostolou M *et al*. XBP1 promotes triple-negative breast cancer by controlling the HIF1alpha pathway. *Nature* 2014; **508**: 103–107.
- 31 Hetz C. The unfolded protein response: controlling cell fate decisions under ER stress and beyond. *Nat Rev Mol Cell Biol* 2012; **13**: 89–102.
- 32 Reineke EL, Benham A, Soibam B, Stashi E, Taegtmeier H, Entman ML *et al*. Steroid receptor coactivator-2 is a dual regulator of cardiac transcription factor function. *J Biol Chem* 2014; **289**: 17721–17731.
- 33 Walter P, Ron D. The unfolded protein response: from stress pathway to homeostatic regulation. *Science* 2011; **334**: 1081–1086.
- 34 Harding HP, Zhang Y, Bertolotti A, Zeng H, Ron D. Perk is essential for translational regulation and cell survival during the unfolded protein response. *Mol Cell* 2000; **5**: 897–904.
- 35 Gupta S, Read DE, Deepti A, Cawley K, Gupta A, Oommen D *et al*. Perk-dependent repression of miR-106b-25 cluster is required for ER stress-induced apoptosis. *Cell Death Dis* 2012; **3**: e333.
- 36 Zhang H, Kuang SQ, Liao L, Zhou S, Xu J. Haploid inactivation of the amplified-in-breast cancer 3 coactivator reduces the inhibitory effect of peroxisome proliferator-activated receptor gamma and retinoid X receptor on cell proliferation and accelerates polyoma middle-T antigen-induced mammary tumorigenesis in mice. *Cancer Res* 2004; **64**: 7169–7177.
- 37 Coste A, Antal MC, Chan S, Kastner P, Mark M, O'Malley BW *et al*. Absence of the steroid receptor coactivator-3 induces B-cell lymphoma. *EMBO J* 2006; **25**: 2453–2464.
- 38 Binet F, Sapielha P. ER stress and angiogenesis. *Cell Metab* 2015; **22**: 560–575.
- 39 Blais JD, Addison CL, Edge R, Falls T, Zhao H, Wary K *et al*. Perk-dependent translational regulation promotes tumor cell adaptation and angiogenesis in response to hypoxic stress. *Mol Cell Biol* 2006; **26**: 9517–9532.
- 40 Gupta S, McGrath B, Cavener DR. PERK regulates the proliferation and development of insulin-secreting beta-cell tumors in the endocrine pancreas of mice. *PLoS One* 2009; **4**: e8008.
- 41 Feng YX, Sokol ES, Del Vecchio CA, Sanduja S, Claessen JH, Proia TA *et al*. Epithelial-to-mesenchymal transition activates PERK-eIF2alpha and sensitizes cells to endoplasmic reticulum stress. *Cancer Disc* 2014; **4**: 702–715.
- 42 Yoshida H, Matsui T, Yamamoto A, Okada T, Mori K. XBP1 mRNA is induced by ATF6 and spliced by IRE1 in response to ER stress to produce a highly active transcription factor. *Cell* 2001; **107**: 881–891.
- 43 Davies MP, Barraclough DL, Stewart C, Joyce KA, Eccles RM, Barraclough R *et al*. Expression and splicing of the unfolded protein response gene XBP-1 are significantly associated with clinical outcome of endocrine-treated breast cancer. *Int J Cancer* 2008; **123**: 85–88.
- 44 Hu R, Warri A, Jin L, Zwart A, Riggins RB, Fang HB *et al*. NF-kappaB signaling is required for XBP1 (unspliced and spliced)-mediated effects on antiestrogen responsiveness and cell fate decisions in breast cancer. *Mol Cell Biol* 2015; **35**: 379–390.
- 45 Wu RC, Qin J, Hashimoto Y, Wong J, Xu J, Tsai SY *et al*. Regulation of SRC-3 (pCIP/ACTR/AIB-1/RAC-3/TRAM-1) coactivator activity by I kappa B kinase. *Mol Cell Biol* 2002; **22**: 3549–3561.
- 46 Gupta A, Hossain MM, Read DE, Hetz C, Samali A, Gupta S. PERK regulated miR-424(322)-503 cluster fine-tunes activation of IRE1 and ATF6 during unfolded protein response. *Sci Rep* 2015; **5**: 18304.
- 47 Gupta A, Read DE, Gupta S. Assays for induction of the unfolded protein response and selective activation of the three major pathways. *Methods Mol Biol* 2015; **1292**: 19–38.
- 48 Cawley K, Logue SE, Gorman AM, Zeng Q, Patterson J, Gupta S *et al*. Disruption of microRNA biogenesis confers resistance to ER stress-induced cell death upstream of the mitochondrion. *PLoS One* 2013; **8**: e73870.



This work is licensed under a Creative Commons Attribution-NonCommercial-NoDerivs 4.0 International License. The images or other third party material in this article are included in the article's Creative Commons license, unless indicated otherwise in the credit line; if the material is not included under the Creative Commons license, users will need to obtain permission from the license holder to reproduce the material. To view a copy of this license, visit <http://creativecommons.org/licenses/by-nc-nd/4.0/>

Supplementary Information accompanies this paper on the Oncogene website (<http://www.nature.com/onc>)